JOURNAL OF CULTURAL ANALYSIS AND SOCIAL CHANGE

Journal of Cultural Analysis and Social Change,
2025, 10(2), 2236-2246
ISSN: 2589-1316

U.S. Economic Policy Uncertainty, Oil Volatility, and Climate Transition After Trump's Withdrawal from the Paris Agreement

Bouthaina Ben Othman [1], Mohamed Essaied Hamrita [2*], Rihab Bedoui Ben Salem [3]

[2] *IHEC Sousse, TUNISIA*; *Email: mhamrita@gmail.com*

*Corresponding Author: mhamrita@gmail.com

Citation: Othman, B. B., Hamrita, M. E. and Salem, R. B. B. (2025). U.S. Economic Policy Uncertainty, Oil Volatility, and Climate Transition After Trump's Withdrawal from the Paris Agreement, *Journal of Cultural Analysis and Social Change*, 10(2), 2236-2246. https://doi.org/10.64753/jcasc.v10i2.1921

Published: November 16, 2025

ABSTRACT

Economic Policy Uncertainty (EPU) captures the unpredictability of government decisions that shape market expectations and investment dynamics. In the energy sector, elevated policy uncertainty amplifies volatility, especially in oil markets where regulatory and geopolitical changes directly influence production, pricing, and trade. Meanwhile, renewable energy markets, represented by indices such as ICLN, respond asymmetrically to policy signals, depending heavily on the consistency of climate commitments and fiscal incentives. This study investigates the multiscale and nonlinear linkages among U.S. EPU, oil market volatility (OVX), and clean energy performance (ICLN). Using a hybrid GARCH–Wavelet–Vine Copula framework with the Maximal Overlap Discrete Wavelet Transform (MODWT), we examine horizon-dependent dependencies across short-, medium-, and long-term frequencies. The proposed model captures both the temporal persistence of volatility and cross-market co-movements driven by policy shocks. Empirical results suggest that surges in U.S. EPU significantly increase oil market volatility and indirectly weaken clean energy stability. Policy reversals, such as the U.S. withdrawal from the Paris Agreement, are found to heighten uncertainty spillovers between oil and renewable markets. The findings highlight that persistent policy uncertainty not only affects investor confidence and portfolio allocation but may also slow the ecological transition by discouraging long-term energy investments.

Keywords: Economic Policy Uncertainty (EPU), Oil Market Volatility (OVX), Clean Energy (ICLN), Wavelet Decomposition; Vine Copula, Volatility Spillovers, Energy Transition.

INTRODUCTION

Economic Policy Uncertainty (EPU) captures the unpredictability of government decisions that shape business activity and financial markets. In the energy sector, rising policy uncertainty heightens volatility, particularly in oil markets where geopolitical and regulatory shifts directly influence supply, pricing, and trade. Renewable energy markets, represented by indices such as ICLN, respond asymmetrically to policy changes, with investor sentiment hinging on the credibility of climate commitments.

Over the past two decades, U.S. energy policy has oscillated between fossil fuel expansion and renewable prioritization. The shale revolution reduced import dependence, while shifting stances on climate agreements—such as the U.S. exit from and reentry into the Paris Accord—intensified uncertainty, affecting both oil and clean energy performance.

Empirical evidence shows that EPU explains a significant share of oil price fluctuations and serves as a forward-looking indicator of volatility. It influences risk perception, stock returns, and cross-market contagion. In contrast, clean energy markets remain highly policy-dependent, responding sharply to fiscal incentives and regulatory consistency. Periods of high EPU or oil market turbulence (e.g., during COVID-19) amplify volatility spillovers between oil and renewables.

Despite extensive research, few studies explore the multiscale, nonlinear interactions linking EPU, oil volatility, and clean energy performance. To fill this gap, this study applies a GARCH–Wavelet–Vine Copula framework using the Maximal Overlap Discrete Wavelet Transform (MODWT) to analyze short- and long-horizon dependencies among U.S. EPU, oil volatility (OVX), and clean energy returns (ICLN).

We hypothesize that rising EPU amplifies oil market volatility and weakens clean energy stability, with long-term implications for investment behavior and the ecological transition. The study addresses how policy shocks propagate across energy markets, influence investor confidence, and shape the pace of the global shift toward sustainable energy.

LITERATURE REVIEW

Economic Policy Uncertainty (EPU) has emerged as a critical factor in explaining financial and commodity market dynamics. Unlike measurable risk, uncertainty arises when future outcomes and their probabilities cannot be estimated precisely (Degiannakis et al. 2018). EPU embodies ambiguity surrounding fiscal, monetary, trade, and regulatory policies, influencing investor confidence, corporate strategies, and macroeconomic stability (Xin Liu et al. 2022). Elevated EPU often leads firms to postpone investment and hiring, dampening growth and reducing expected returns (Bloom 2009; Kang et al. 2014; Kang and Ratti 2017b; Boako and Liu 2017). It also induces risk aversion among investors, heightening market volatility and weakening sentiment (Hansen 1999). The introduction of the EPU index by Baker, Bloom, and Davis (Baker, Bloom, and Davis 2016) provided an empirical basis for quantifying policy-related uncertainty, stimulating extensive global research.

Oil markets are particularly sensitive to policy uncertainty. Beyond geopolitical and supply–demand factors (Henriques and Sadorsky 2008), EPU constitutes a persistent source of price volatility. Studies show that fluctuations in EPU explain a significant share of oil price variations, with both demand- and supply-side shocks contributing (Kang and Ratti 2013, 2017c, 2017a). Multiscale analyses confirm that EPU consistently leads oil futures volatility across different horizons (Yang et al. 2019; Dai, Wang, and Zhou 2020; Sum and al. 2012). By shaping expectations and risk tolerance, EPU amplifies oil market volatility and transmits uncertainty across financial markets (Liang et al. 2020; Xin Liu et al. 2022; X. Liu et al. 2023). Cross-country evidence further indicates that EPU in oil-importing nations predicts long-term price trends (Su et al. 2021; Wang et al. 2022a).

The rise of renewable and clean energy markets introduces new policy-driven dynamics. These markets depend heavily on subsidies, tax incentives, and regulatory clarity (Managi et al. 2013). Clean energy returns co-move with oil prices but exhibit asymmetric reactions to policy shocks (Henriques and Sadorsky 2008). Climate-related uncertainty—such as delays in international agreements—exerts disproportionate pressure on renewable assets (Wang and al. 2022; Zhang and al. 2023; Chen, Zhu, and Liu 2025). Oil volatility (OVX) also significantly affects clean energy equity prices (Dutta and al. 2017), especially during crises when market connectedness intensifies (Foglia et al. 2020).

Systemic risk research reveals time-varying and asymmetric dependencies between oil and renewables, often driven by oil price dynamics (Reboredo 2015, 2018). Real activity indicators also predict clean energy volatility more effectively than textual uncertainty measures (Wang et al. 2022b).

Overall, the literature portrays EPU as both a source and a transmission channel of volatility across oil and clean energy markets. However, few studies address their multiscale, nonlinear interdependencies. Advanced approaches, such as wavelet decomposition and vine copula models, offer promising avenues to uncover how policy uncertainty, oil volatility, and clean energy performance interact across time horizons—yielding insights for investors, policymakers, and the energy transition.

METHODOLOGY

This study employs a multiscale modeling approach combining the Maximal Overlap Discrete Wavelet Transform (MODWT), ARMA–GARCH modeling, and vine copula estimation to investigate the dynamic dependence among U.S. economic policy uncertainty (EPU), oil market volatility (OVX), and clean energy performance (ICLN). The MODWT decomposes each log-return series into components capturing short-, medium-, and long-term fluctuations while preserving alignment with the original data. Each wavelet component is then modeled using an ARMA–GARCH(1,1) specification to account for linear dependencies and conditional heteroscedasticity, with standardized residuals extracted for copula analysis. These residuals are transformed to uniform margins and fitted to candidate bivariate copulas, which are subsequently combined into a vine copula structure (C-vine or D-vine) to capture complex, potentially asymmetric dependencies, including tail behavior. Model selection is guided by log-likelihood and information criteria, and goodness-of-fit tests ensure adequacy.

This integrated framework allows for a detailed assessment of how policy uncertainty propagates across oil and clean energy markets over multiple time horizons.

Wavelet Transform and Decomposition Approch

Wavelet transformation is a mathematical technique used to decompose a signal or time series into different components at multiple resolution levels. This method captures long-memory volatility and structural changes, improving forecasting models. Unlike traditional Fourier analysis, wavelet transforms provide localized time-frequency representation, making them effective for non-stationary time series like financial data.

Wavelet decomposition recursively applies low-pass and high-pass filters, separating high-frequency components from low-frequency ones. This enhances the ability to detect mildly explosive bubbles and other structural changes in time series data. Wavelet transforms are widely used in finance, engineering, hydrology, and medicine due to their ability to analyze signals at different time scales.

The wavelet decomposition of a time series $r(t)$ can be expressed as:

$$r(t) = \sum_k s_{J,k}\, \Phi_{J,k}(t) + \sum_k d_{J,k}\, \phi_{J,k}(t) + \sum_k d_{J-1,k}\, \phi_{J-1,k}(t) + \cdots + \sum_k d_{1,k}\, \phi_{1,k}(t)$$

where:

- $\Phi_{J,k}(t)$ and $\phi_{j,k}(t)$ are scaling (father) and wavelet (mother) functions.

- j represents the resolution level.

- k is the index of coefficients at each scale.

- $s_{J,k}$ are the scaling coefficients, capturing low-frequency trends.

- $d_{j,k}$ are the wavelet coefficients, capturing high-frequency details.

The orthogonal basis functions for the father and mother wavelets are:

$$\Phi_{j,k}(t) = 2^{\frac{-j}{2}} \Phi\left(\frac{t - 2^j k}{2^j}\right)$$

$$\phi_{j,k}(t) = 2^{\frac{-j}{2}} \phi\left(\frac{t - 2^j k}{2^j}\right)$$

The scaling and wavelet coefficients are computed as:

$$s_{j,k} = \int r(t)\Phi_{j,k}(t)dt$$

$$d_{j,k} = \int r(t)\phi_{j,k}(t)dt, j = 1,2, \dots, J$$

The multi-scale decomposition results in:

$$R(t) = S_J + D_J + D_{J-1} + \cdots + D_1$$

where:

- S_J represents the smooth, low-frequency part of the signal.
- D_j represents the detail, high-frequency components at scale j.

This complete wavelet decomposition provides a multi-scale analysis of time series data, useful for detecting patterns, anomalies, and long-term trends.

Vine Copula–GARCH Framework

The multivariate **Vine Copula–GARCH** approach extends the bivariate copula-GARCH model to higher dimensions, allowing flexible modeling of complex dependencies across multiple financial assets. This framework captures:

Marginal Volatility Dynamics using ARMA–GARCH models.

Nonlinear and Tail Dependencies using vine copulas (C-vine and D-vine).

Vine copulas provide a hierarchical structure based on pair-copula constructions (PCC), introduced by Bedford and Cooke (2001, 2002). Two commonly used structures are:

- **C-vine**: a central node connects to all other variables in each tree.
- **D-vine**: variables are connected sequentially, forming a path-like structure.

Marginal Modeling with GARCH

Let (R_{t,s}) denote the return series at time (t) and scale (s). The ARMA–GARCH model is:

Mean Equation:

$$R_{t,s} = a_{0,s} + \sum_{i=1}^{m} a_{i,s} R_{t-i,s} + \sum_{i=1}^{n} b_{i,s} \varepsilon_{t-i,s} + \varepsilon_{t,s},$$

Variance Equation:

$$h_{t,s} = \omega + \sum_{j=1}^{p} \beta_{j,s} h_{t-j,s} + \sum_{i=1}^{q} \alpha_{i,s} \varepsilon_{t-i,s}^{2},$$

with $\varepsilon_{t,s} = z_t\sqrt{h_{t,s}}$, where (z_t) is a standard white noise process. Standardized residuals $\hat{z} * t, s = \varepsilon * t, s/\sqrt{h_{t,s}}$ are used in copula modeling.

Vine Copula Construction

C-Vine Copula

A C-vine copula has a central node that connects with all others. For (d)-dimensional variables, the joint density is:

$$f(x_1, \dots, x_d) = \prod_{k=1}^{d} f_k(x_k) \prod_{h=2}^{d} c_{1,h}\left(F_1(x_1), F_h(x_h)\right) \prod_{j=2}^{d-1} \prod_{i=1}^{d-j} c_{j,j+i|1:(j-1)}\left(F\left(x_j|x_1, \dots, x_{j-1}\right), F\left(x_{j+i}|x_1, \dots, x_{j-1}\right)\right),$$

where:

- $f_k(x_k)$ are marginal densities.
- $c_{j,j+i|1:(j-1)}$ are conditional copula densities.

Example: 4-dimensional C-vine decomposition:

$$f(x_1, x_2, x_3, x_4) \quad f_1(x_1) f_2(x_2) f_3(x_3) f_4(x_4) \cdot c_{1,2}(F_1, F_2) c_{1,3}(F_1, F_3) c_{1,4}(F_1, F_4)$$

D-Vine Copula

A D-vine copula arranges variables in a sequential path. Its joint density is:

$$f(x_1, \dots, x_d) \quad \prod_{k=1}^{d} f_k(x_k) \prod_{h=1}^{d-1} c_{h,h+1}\left(F_h(x_h), F_{h+1}(x_{h+1})\right) \prod_{j=2}^{d-1} \prod_{i=1}^{d-j} c_{i,i+j|i+1:,i+j-1}\left(F\left(x_i|x_{i+1}, \dots, x_{i+j-1}\right),\right.$$

Example: 4-dimensional D-vine decomposition:

$$f(x_1, x_2, x_3, x_4) \quad f_1(x_1) f_2(x_2) f_3(x_3) f_4(x_4) \dots c_{1,2}(F_1, F_2) c_{2,3}(F_2, F_3) c_{3,4}(F_3, F_4)$$

Estimation Procedure

Following Czado et al. (2012), sequential estimation is applied:

- Estimate unconditional pair-copulas in the first tree.
- Use them to estimate conditional pair-copulas in the second tree.
- Repeat until all pair-copulas are estimated.

These sequential estimates are then used as starting values for Maximum Likelihood Estimation (MLE) to refine parameter estimates.

For C-vine, the log-likelihood is:

$$lnL = \sum_{i=1}^{T} \sum_{j=1}^{d-1} \sum_{k=1}^{d-j} ln\, c_{j,j+k|1:(j-1)}\left(F\left(u_{i,j}|u_{i,1}, \dots, u_{i,j-1}\right), F\left(u_{i,j+k}|u_{i,1}, \dots, u_{i,j-1}\right)|\theta_{j,j+k|1:(j-1)}\right),$$

and similarly for D-vine:

$$lnL = \sum_{i=1}^{T}\sum_{j=1}^{d-1}\sum_{k=1}^{d-j} ln\, c_{i,i+k|i+1:,i+k-1}\left(F\left(u_{i,i}|u_{i,i+1},\dots,u_{i,i+k-1}\right),F\left(u_{i,i+k}|u_{i,i+1},\dots,u_{i,i+k-1}\right)|\theta_{i,i+k|i+1:,i+k-1}\right).$$

This Vine Copula–GARCH framework allows modeling of both marginal volatility dynamics and high-dimensional dependence, including asymmetric tail behavior and dynamic correlations among financial assets.

DATA AND EMPIRICAL RESULTS

Data Description

The empirical analysis is based on daily data covering the period from February 17, 2014, to September 12, 2025. Three time series are considered to capture the dynamics between economic policy uncertainty, oil market volatility, and renewable energy markets.

U.S. Economic Policy Uncertainty (USEPU): The daily U.S. economic policy uncertainty index is obtained from Baker, Bloom, and Davis (2016). It reflects the frequency of news articles containing terms related to the economy, policy, and uncertainty. The series is not a traded asset but serves as a proxy for shifts in policy-related uncertainty.

Crude Oil Volatility Index (OVX): The CBOE Crude Oil Volatility Index (^OVX) is retrieved from Yahoo Finance. OVX measures the market's expectation of 30-day volatility in crude oil prices, derived from option prices on the United States Oil Fund (USO). It serves as a forward-looking indicator of oil market risk.

Renewable Energy Market (ICLN): The iShares Global Clean Energy ETF (ICLN) is obtained from Yahoo Finance. The ETF tracks the performance of global companies in the clean energy sector and is used as a proxy for renewable energy market performance. Adjusted daily closing prices are used.After preliminary analysis of the data, a total of 4216 observations of the tree effective data variables were selected. To facilitate analysis of volatility and dependence structures, we compute logarithmic returns as:

$$R_t = 100 \times ln\left(\frac{P_t}{P_{t-1}}\right),$$

where P_t denotes the adjusted price or index value at time t. The final dataset consists of both the level series (USEPU, OVX, ICLN) and their corresponding daily log returns (Ret_{USEPU}, Ret_{OVX}, Ret_{ICLN}).

This dataset provides a coherent framework for examining the interaction between policy uncertainty, oil market volatility, and renewable energy markets across different time horizons.

Descriptive Statistics

Descriptive Statistics of Return Series

	Mean	**Std_Dev**	**Median**	**Max**	**Min**	**Skewness**	**Kurtosis**
Ret_USEPU	0.0303	55.4793	-0.8427	389.2211	-348.3855	0.0894	2.7736
Ret_OVX	0.0162	4.9258	-0.0414	47.5063	-62.2251	0.4991	17.0109
Ret_ICLN	0.0144	1.3703	0.0000	10.7998	-13.7093	-0.2336	8.1888

The preliminary analysis reveals distinct distributional properties across the three return series. Descriptive statistics from (table.1) show that Ret_USEPU is the most volatile, with extreme fluctuations but near symmetry, while Ret_OVX exhibits moderate volatility with strong fat tails and positive skewness, and Ret_ICLN displays the lowest volatility yet is characterized by negative skewness and leptokurtosis. Stationarity is confirmed by the ADF and KPSS tests, whereas the Jarque–Bera test rejects normality in all cases, consistent with excess kurtosis. Histogram (Appendix A) patterns further highlight deviations from Gaussian behavior, with Ret_USEPU showing wide dispersion, Ret_OVX being sharply centered but heavy-tailed, and Ret_ICLN remaining concentrated yet asymmetric. Collectively, these results establish clear evidence of non-Gaussian distributions across the series, justifying the use of GARCH-type models with flexible error structures in subsequent analysis.

Series Wavelet Decomposition

Following prior studies, we use a seven-level wavelet decomposition to capture the multiscale dynamics of return and volatility series. This approach aligns with Rua and Nunes (2009), Vacha and Barunik (2012), and Bouri et al. (2020), who apply six to eight levels in financial and energy market analysis.
Each decomposition level corresponds to a different investment horizon:

- Levels d_1–d_3 capture short-term fluctuations (2–16 days)
- Levels d_4–d_5 capture medium-term dynamics (16–64 days)
- Levels d_6–d_7 capture long-term trends (64–256 days)

A seven-level structure allows clear separation between high-frequency noise, cyclical patterns, and low-frequency components, improving the detection and interpretation of time-varying dependence. This choice is feasible because the daily dataset meets the minimum observation requirement of $2^7 = 128$ points.

Descriptive Statistics for Sub-Series

Descriptive Statistics for All Subseries

Series	Mean	SD	Min	Max	Median	Skewness	Kurtosis
short_USEPU	0	55.213706	-345.753151	389.428545	-0.6051453	0.0813482	2.7815687
med_USEPU	0	3.7638871	-12.313646	17.9142267	-0.0591295	0.1630293	0.6164154
long_USEPU	0	0.8549174	-2.430818	3.5714171	-0.0234341	0.4608542	1.3023812
short_OVX	0	4.5719469	-53.950882	38.7177267	0.0438651	-0.0234266	13.687115
med_OVX	0	1.3675901	-6.401651	10.0679239	-0.0478372	0.7149425	5.5291569
long_OVX	0	0.5490855	-2.053949	3.3919171	-0.0522101	0.9354959	6.0595005
short_ICLN	0	1.2547701	-9.824612	9.5205218	-0.0076723	0.1219288	6.8531528
med_ICLN	0	0.3800907	-2.823573	1.9688302	-0.0031330	-0.2548979	4.4410467
long_ICLN	0	0.2116951	-1.060104	0.6509976	0.0002806	-0.4922906	2.6759936

The sub-series exhibit substantial variation across horizons and indices. Short-term series show the largest standard deviations, particularly short_USEPU and short_OVX, reflecting higher volatility at high frequencies. Skewness is generally small, though long_ICLN and medium/long OVX show slight negative or positive asymmetry. Kurtosis is elevated for several series, especially short_OVX and short_ICLN, indicating heavy tails and a higher likelihood of extreme observations. Overall, the statistics suggest that volatility and tail behavior decrease with increasing time horizon, consistent with aggregation effects in financial and policy-related series.

Diagnostic Tests for Sub-Series

Statistical Tests for Sub-Series

Series	ADF_p	KPSS_p	JB_p	Hurst	GPH_d	BDS_stat	BDS_p	Shapiro_p
short_USEPU	0.01	0.1	0	0.2774	-3.1064	7.9495	0	0
medium_USEPU	0.01	0.1	0	0.4350	-6.7135	280.1849	0	0
long_USEPU	0.01	0.1	0	0.5941	-3.2599	337.5874	0	0
short_OVX	0.01	0.1	0	0.3572	-5.7924	22.3795	0	0
medium_OVX	0.01	0.1	0	0.4807	-6.8456	223.2727	0	0
long_OVX	0.01	0.1	0	0.6400	-3.2398	357.6153	0	0
short_ICLN	0.01	0.1	0	0.3146	-3.6430	18.2991	0	0
medium_ICLN	0.01	0.1	0	0.4971	-6.8686	211.8837	0	0
long_ICLN	0.01	0.1	0	0.6049	-3.4849	329.3591	0	0

Preliminary tests reveal important characteristics of the decomposed series. The ADF, KPSS, and PP results jointly confirm stationarity across all scales, validating subsequent dependence modeling. The Hurst exponent indicates scale-dependent behavior: short-term anti-persistence ($H < 0.5$), near-random dynamics at medium horizons, and long-term persistence ($H > 0.6$). Thus, shocks dissipate quickly in the short run but accumulate over time. The fractional differencing parameter (GPH) broadly aligns with these findings, reinforcing evidence of long memory at extended horizons. The BDS test rejects i.i.d. behavior across all scales, confirming strong nonlinear dependence. Overall, the series are stationary yet exhibit scale-dependent persistence and nonlinearities, supporting the application of nonlinear volatility models such as GARCH-type frameworks.

ARMA-GARCH Filtering Specification

Volatility dynamics were modeled using autoregressive (AR) and generalized autoregressive conditional heteroskedasticity (GARCH) frameworks, selected through information criteria and residual diagnostics. The approach was tailored to capture short-, medium-, and long-term horizons consistent with each series' persistence characteristics. For short and medium terms, nonlinear specifications—particularly eGARCH and GJR-GARCH—best fit the log-differenced data, effectively modeling conditional heteroskedasticity indicated by significant ARCH effects. Diagnostic tests (Jarque–Bera, Shapiro–Wilk, Ljung–Box) confirmed model adequacy, while standardized Student's t and skewed t distributions provided superior fits for heavy-tailed returns based on AIC/BIC criteria. At longer horizons, volatility clustering diminished, and a simple AR(1) model sufficiently described the dynamics, as additional GARCH components offered negligible improvement. Overall, the results support a horizon-dependent modeling strategy: nonlinear GARCH-type models are crucial for short- and medium-term volatility, whereas linear AR structures adequately capture long-term stability.

Multivariante Dependence Structure MOdeling (Vine-Copula)

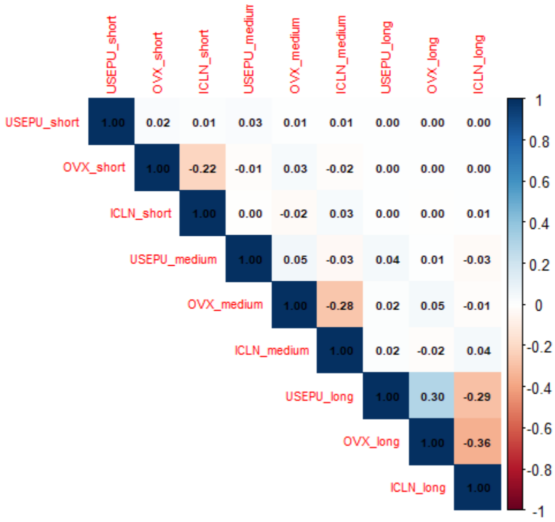

Spearman Cross-Horizon Correlation Matrix

The analysis of Spearman rank correlations across time horizons indicates that dependence is predominantly contemporaneous and strongest within identical horizons. Long-horizon components exhibit the highest correlation magnitudes, with $\rho_{ICLN-OVX} = -0.368$, $\rho_{OVX-USEPU} = 0.305$, and $\rho_{ICLN-USEPU} = -0.287$. Correlations at medium and short horizons remain positive but comparatively weaker, while cross-horizon correlations are consistently low, ranging between -0.025 and0.02. These results suggest limited intertemporal co-movement across horizons. Accordingly, modeling dependence structures using vine copulas is most meaningful within individual horizons, where the relationships among EPU, oil volatility, and clean energy performance are statistically robust and economically interpretable.

Estimating One Vine Per Horizon

Structure Selection

Kendall's Tau Matrices for All Horizons

	Variable	USEPU	OVX	ICLN	Sum_abs
	=== SHORT HORIZON ===	NA	NA	NA	NA
USEPU	USEPU	1.000	0.014	0.008	1.023
OVX	OVX	0.014	1.000	-0.148	1.162
ICLN	ICLN	0.008	-0.148	1.000	1.157
	=== MEDIUM HORIZON ===	NA	NA	NA	NA

USEPU	USEPU	1.000	0.035	-0.023	1.057
OVX	OVX	0.035	1.000	-0.191	1.225
ICLN	ICLN	-0.023	-0.191	1.000	1.213
	=== LONG HORIZON ===	NA	NA	NA	NA
USEPU	USEPU	1.000	0.208	-0.201	1.408
OVX...11	OVX	0.208	1.000	-0.248	1.456
ICLN...12	ICLN	-0.201	-0.248	1.000	1.449

The analysis of Kendall's Tau across multiple horizons reveals a clear evolution in dependence between sub-series variables. In the short term, relationships are weak, with minimal influence of USEPU on OVX and ICLN. At the medium horizon, USEPU begins to impact oil volatility, while the negative association between OVX and ICLN strengthens, suggesting emerging substitution or hedging effects. In the long term, dependence intensifies: USEPU strongly drives OVX, and both OVX and USEPU exert negative effects on ICLN, highlighting the vulnerability of clean energy markets to sustained policy uncertainty and oil market risks.

we further, construct scatterplot matrices for each horizon. Using Pearson correlations, the matrices display bivariate relationships, marginal distributions, and density estimates, while overlayed ellipses highlight the shape, orientation, and potential asymmetry of joint distributions. The ellipses provide a visual indication of correlation strength and direction, making deviations from linearity or the presence of outliers easier to detect.

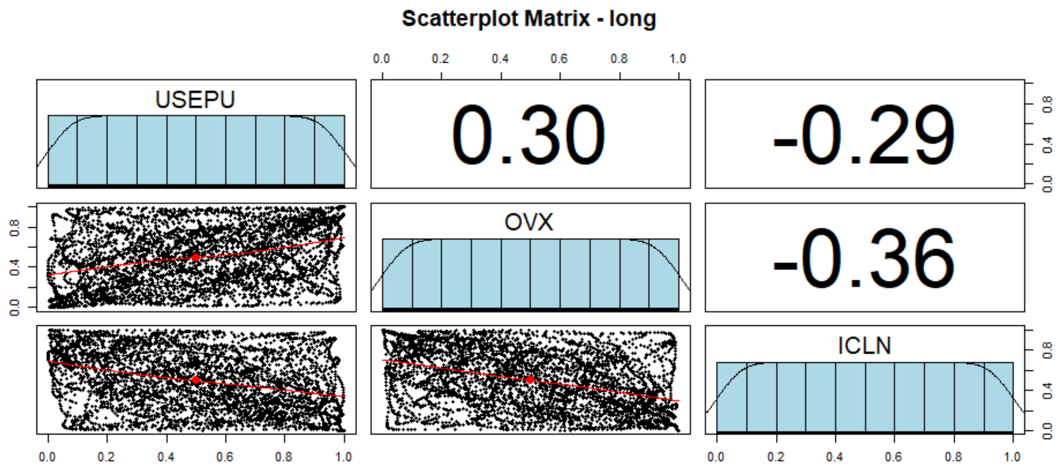

To examine the dependence structure among the selected financial series, we first transformed the standardized residuals of each series into uniform variables on the interval $[0,1]$ through the probability integral transform. This step ensured the uniform margins necessary for copula-based modeling. For each time horizon-short, medium, and long, we constructed both C-vine and D-vine copula models. The ordering of variables in each structure was determined by empirical Kendall's τ. In the C-vine, the variable with the highest sum of absolute Kendall's τ with all others served as the root node, while in the D-vine, variables were ordered sequentially in descending order of pairwise Kendall's τ.

In the C-vine, the first tree connects the root variable to all others, and subsequent trees capture conditional dependencies among the remaining variables. In the D-vine, variables are connected sequentially, with higher-order trees modeling conditional dependence structures. Each pairwise dependence was modeled using a wide range of copula families, including Gaussian, Student-t, Clayton, Frank, Gumbel, Joe, and their rotated variants. Pair copulas were first estimated sequentially using maximum likelihood, and the family with the lowest Akaike Information Criterion (AIC) was selected for each pair. The full vine structure was then re-estimated using maximum likelihood to obtain final parameters, denoted as θ for single-parameter copulas and ν for two-parameter copulas.

For each pair, the empirical Kendall's τ was calculated from the uniformized data, and the upper and lower tail dependence coefficients (λ_U and λ_L) were estimated as the proportion of simultaneous extreme co-movements in the corresponding tails. Model fit was further assessed using log-likelihood, AIC, BIC, and the number of estimated parameters. The model with the lowest AIC for each horizon was retained as the best-fitting vine. The final results report, for each pair, the selected copula family, estimated parameters, empirical Kendall's τ, and tail dependence coefficients.

Results of Estimated Parameters for the C-Vine and D-Vine Copula

	Horizon	VineType	Tree	Pair	ConditioningSet	Family	θ	ν	τ	λU	λL
lambdaU	short	C-Vine	Tree 1	USEPU-OVX	NA	clayton	0.0289659	NA	0.0142762	0.0026005	0.0016548
lambdaU1	short	C-Vine	Tree 1	USEPU-ICLN	NA	gumbel	1.0084562	NA	0.0083853	0.0023641	0.0018913
lambdaU2	short	C-Vine	Tree 2	OVX-ICLN	USEPU	t	-0.2313001	5.561693	-0.1481858	0.0014184	0.0035461
lambdaU3	short	D-Vine	Tree 1	USEPU-OVX	NA	t	-0.2306733	5.604455	0.0142762	0.0026005	0.0016548
lambdaU11	short	D-Vine	Tree 1	OVX-ICLN	NA	gumbel	1.0084562	NA	-0.1481858	0.0014184	0.0035461
lambdaU21	short	D-Vine	Tree 2	USEPU-ICLN	OVX	clayton	0.0352202	NA	0.0083853	0.0023641	0.0018913
lambdaU4	medium	C-Vine	Tree 1	USEPU-OVX	NA	gaussian	0.0542100	NA	0.0345281	0.0040189	0.0026005
lambdaU12	medium	C-Vine	Tree 1	USEPU-ICLN	NA	gaussian	-0.0355166	NA	-0.0226153	0.0026005	0.0026005
lambdaU22	medium	C-Vine	Tree 2	OVX-ICLN	USEPU	gumbel	1.2349796	NA	-0.1905254	0.0007092	0.0007092
lambdaU31	medium	D-Vine	Tree 1	USEPU-OVX	NA	gumbel	1.2353692	NA	0.0345281	0.0040189	0.0026005
lambdaU111	medium	D-Vine	Tree 1	OVX-ICLN	NA	gaussian	-0.0355166	NA	-0.1905254	0.0007092	0.0007092
lambdaU211	medium	D-Vine	Tree 2	USEPU-ICLN	OVX	gaussian	0.0469400	NA	-0.0226153	0.0026005	0.0026005
lambdaU5	long	C-Vine	Tree 1	USEPU-OVX	NA	t	0.3206304	4.811248	0.2077895	0.0087470	0.0134752
lambdaU13	long	C-Vine	Tree 1	USEPU-ICLN	NA	t	-0.3099325	7.290980	-0.2006129	0.0000000	0.0000000
lambdaU23	long	C-Vine	Tree 2	OVX-ICLN	USEPU	t	-0.3211890	7.237839	-0.2484631	0.0016548	0.0021277
lambdaU32	long	D-Vine	Tree 1	USEPU-OVX	NA	t	-0.3804519	4.032660	0.2077895	0.0087470	0.0134752
lambdaU112	long	D-Vine	Tree 1	OVX-ICLN	NA	t	-0.3099325	7.290980	-0.2484631	0.0016548	0.0021277
lambdaU212	long	D-Vine	Tree 2	USEPU-ICLN	OVX	t	0.2322667	9.686227	-0.2006129	0.0000000	0.0000000

The vine copula analysis reveals horizon-dependent dependence among USEPU, OVX, and ICLN. For the short-term horizon, the C-vine is the best-fitting model, identifying USEPU as the central variable. Dependence is weakly positive between USEPU and OVX ($\tau \approx 0.015$, Clayton copula) and between USEPU and ICLN ($\tau \approx 0.006$, Gumbel copula), while OVX and ICLN exhibit moderate negative dependence ($\tau \approx -0.148$, Student-t copula). Tail dependence is minimal, indicating limited simultaneous extreme co-movements.

At medium horizons, the D-vine provides a better fit, capturing stronger bilateral links: USEPU–OVX ($\tau \approx 0.040$, Gumbel) and OVX–ICLN ($\tau \approx -0.190$, Gaussian), with low tail dependence reflecting rare joint extremes. At long horizons, the D-vine again outperforms the C-vine, revealing more pronounced dependence: USEPU–OVX ($\tau \approx 0.208$, Student-t copula) and OVX–ICLN ($\tau \approx -0.252$, Student-t copula), with measurable upper and lower tail coefficients consistent with the heavy-tailed nature of the t copulas.

Overall, the choice of copula families highlights the asymmetry and tail behavior of the dependencies: Clayton and Gumbel copulas capture lower and upper tail concentration, respectively, while Student-t copulas account for symmetric extreme co-movements. Across all horizons, USEPU consistently emerges as the most influential variable, and both energy and clean energy markets display increasing sensitivity to policy-driven shocks over longer periods.

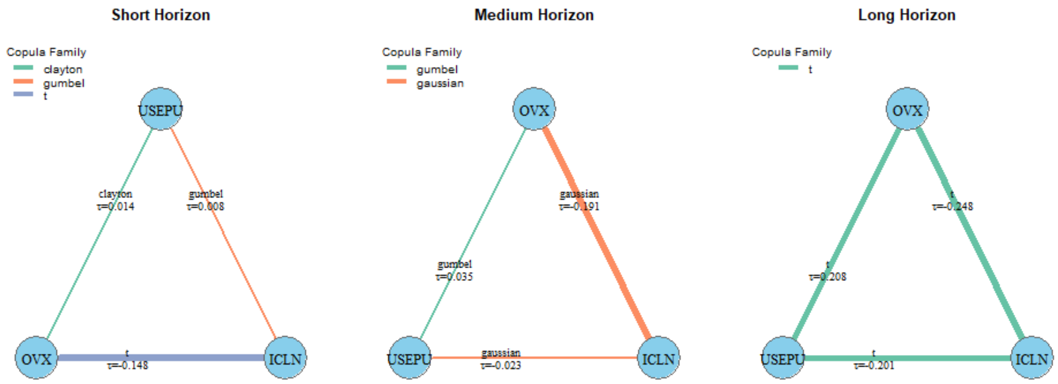

The dependence among policy uncertainty, oil volatility, and clean energy markets varies across investment horizons. At short horizons, the dependence between USEPU and OVX is weakly positive ($\tau = 0.016$), the relationship between USEPU and ICLN is nearly independent ($\tau = 0.007$), and the conditional dependence between OVX and ICLN given USEPU is moderately negative ($\tau = -0.148$), indicating rapid oil market reactions to EPU shocks while clean energy remains relatively insulated.

At medium horizons, dependence strengthens: USEPU–OVX ($\tau = 0.043$), OVX–ICLN ($\tau = -0.190$), and USEPU–ICLN ($\tau = -0.033$), reflecting the reinforcement of oil volatility by policy uncertainty and the presence of counter-movements in clean energy assets.

Long-term horizons display substantial dependence: USEPU–OVX ($\tau = 0.209$, $\lambda_U = 0.009$, $\lambda_L = 0.014$) and OVX–ICLN ($\tau = -0.258$), highlighting amplified oil market risks and weakened clean energy performance under sustained policy uncertainty.

C-vine and D-vine analyses jointly show the persistence of EPU shocks, asymmetric clean energy responses, and the vulnerability of energy markets to prolonged uncertainty, emphasizing the importance of stable climate and energy policies to reduce spillovers and support investor confidence.

Discussion and Policy Implications

Persistent U.S. economic policy uncertainty (EPU) exerts a pronounced influence on energy market volatility, particularly amplifying fluctuations in the oil volatility index (OVX). Short-term policy shocks transmit rapidly to oil markets, reflecting the sector's sensitivity to fiscal, regulatory, and geopolitical signals. In contrast, clean energy markets (ICLN) exhibit a more gradual response, with effects emerging over medium and long horizons as policy uncertainty erodes investor confidence and project financing stability. Over time, this asymmetry gives rise to an increasingly negative dependence between oil and clean energy returns, implying that sustained policy inconsistency undermines market equilibrium and cross-sectoral diversification.

Historical events, such as the U.S. withdrawal from the Paris Agreement, demonstrate how abrupt policy reversals exacerbate volatility spillovers, disrupt renewable investment flows, and destabilize risk perceptions. Such uncertainty deters both traditional and green energy investment, constraining portfolio rebalancing and slowing capital inflows into low-carbon technologies. Consequently, the ecological transition becomes more fragile, as persistent uncertainty weakens incentives for innovation, infrastructure expansion, and long-term energy planning.

The joint dynamics between EPU and oil price volatility underscore their central role in shaping clean energy performance. Mitigating policy uncertainty—through consistent climate commitments, regulatory transparency, and stable fiscal incentives—is therefore essential for managing systemic energy risks, sustaining investor confidence, and accelerating the transition toward a resilient, low-carbon economy.

CONCLUSION

This study provides a comprehensive analysis of the multiscale dependence between U.S. economic policy uncertainty, oil market volatility, and clean energy market dynamics. Using vine copula models across short, medium, and long-term horizons, we demonstrate that policy uncertainty exerts both immediate and persistent effects on energy markets. Short-term shocks primarily impact oil volatility, while clean energy markets exhibit delayed responses. Over longer horizons, prolonged policy inconsistency strengthens negative dependencies between oil and renewable assets, highlighting the vulnerability of clean energy investments under uncertain economic policies. Our findings emphasize that unpredictable policy decisions, including major events like the U.S. withdrawal from the Paris Agreement, can undermine market stability, impede long-term investment in both oil and renewable energy, and slow the pace of the ecological transition. These results underscore the need for stable, consistent climate and energy policies to mitigate uncertainty spillovers, enhance investor confidence, and foster a smooth and timely transition toward a low-carbon economy.

REFERENCES

Baker, Scott R., Nicholas Bloom, and Steven J. Davis. 2016. "Measuring Economic Policy Uncertainty." *The Quarterly Journal of Economics* 131 (4): 1593–1636. https://doi.org/10.1093/qje/qjw024.

Bloom, Nicholas. 2009. "The Impact of Uncertainty Shocks." *SSRN Scholarly Paper*, no. 1014334.

Boako, G., and H. Liu. 2017. "Economic Policy Uncertainty and Investment." *Journal of Economic Studies* 44: 580–601.

Chen, Y., H. Zhu, and Y. Liu. 2025. "Measuring Multi-Scale Risk Contagion Between Crude Oil, Clean Energy, and Stock Market: A MODWT-Vine-Copula Method." *Research in International Business and Finance* 75: 102790.

Dai, X., Q. Wang, and D. Zhou. 2020. "Multi-Scale Dependence Structure and Risk Contagion Between Oil, Gold, and US Exchange Rate." *Energy Economics* 88: 104774. https://doi.org/10.1016/j.eneco.2020.104774.

Degiannakis, Stavros et al. 2018. "Economic Policy Uncertainty and Stock Market Volatility." *Journal of Financial Stability* 35: 45–60. https://doi.org/10.1016/j.jfs.2018.05.004.

Dutta, A., and et al. 2017. "Oil Volatility and Clean Energy Returns." *Energy Economics* 66: 115–24.

Foglia, A. et al. 2020. "Connectedness of Energy Markets During COVID-19." *Energy Policy* 144: 111641.

Hansen, B. E. 1999. "Threshold Effects in Non-Dynamic Panels: Estimation, Testing, and Inference." *Journal of Econometrics* 93: 345–68.

Henriques, I., and P. Sadorsky. 2008. "The Impact of Electricity Prices on Clean Energy Stock Returns." *Energy Economics* 30: 998–1011.

Kang, W. et al. 2014. "Economic Policy Uncertainty and Oil Price Volatility." *Energy Economics* 44: 62–70.

Kang, W., and R. A. Ratti. 2013. "Oil Price Volatility and Economic Policy Uncertainty." *Energy Economics* 39: 44–55.

———. 2017a. "Policy Uncertainty and Commodity Market Spillovers." *Resources Policy* 52: 12–22.

———. 2017b. "Policy Uncertainty and Commodity Prices." *Journal of International Money and Finance* 70: 1–12.

———. 2017c. "The Effects of Policy Uncertainty on Oil Prices." *Energy Journal* 38: 121–42.

Liang, H. et al. 2020. "Policy Uncertainty and Energy Market Returns." *Energy Policy* 137: 111074.

Liu, X. et al. 2023. "Energy Market Volatility and Policy Shocks." *Energy Economics* 124: 107586.

Liu, Xin et al. 2022. "Economic Policy Uncertainty and Energy Market Dynamics." *Energy Economics* 110: 105956. https://doi.org/10.1016/j.eneco.2022.105956.

Managi, S. et al. 2013. "Clean Energy Market Dynamics and Policy Uncertainty." *Renewable Energy* 50: 68–75.

Reboredo, J. C. 2015. "Oil and Renewable Energy Stock Dependence." *Energy Economics* 48: 199–208.

———. 2018. "Energy Market Dependence and Tail Risks." *Journal of Commodity Markets* 11: 1–15.

Su, C. W. et al. 2021. "Policy Uncertainty and Oil Price Dynamics." *Energy Economics* 101: 105402.

Sum, V., and et al. 2012. "Economic Policy Uncertainty and Stock Market Volatility." *Journal of Financial Economics* 104: 122–38.

Wang, Y. et al. 2022a. "Economic Policy Uncertainty and Oil Market Volatility." *Resources Policy* 77: 102626.

——— et al. 2022b. "Real Economic Activity and Clean Energy Volatility." *Energy Policy* 165: 112933.

Wang, Y., and et al. 2022. "Climate Policy Uncertainty and Clean Energy Returns." *Energy Economics* 112: 106156.

Yang, J. et al. 2019. "Economic Policy Uncertainty and Oil Market Volatility: Evidence from China." *Energy Economics* 83: 210–24.

Zhang, L., and et al. 2023. "Renewable Energy Markets and Policy Shocks." *Renewable Energy* 194: 202–15.

